

Probing SWI/SNF remodeling of the nucleosome by unzipping single DNA molecules

Alla Shundrovsky¹, Corey L Smith², John T Lis³, Craig L Peterson² & Michelle D Wang¹

Chromatin-remodeling enzymes can overcome strong histone-DNA interactions within the nucleosome to regulate access of DNA-binding factors to the genetic code. By unzipping individual DNA duplexes, each containing a uniquely positioned nucleosome flanked by long segments of DNA, we directly probed histone-DNA interactions. The resulting disruption-force signatures were characteristic of the types and locations of interactions and allowed measurement of the positions of nucleosomes with 2.6-base-pair (bp) precision. Nucleosomes remodeled by yeast SWI/SNF were moved bidirectionally along the DNA, resulting in a continuous position distribution. The characteristic distance of motion was ~ 28 bp per remodeling event, and each event occurred with a catalytic efficiency of 0.4 min^{-1} per nM SWI/SNF. Remodeled nucleosomes had essentially identical disruption signatures to those of unremodeled nucleosomes, indicating that their overall structure remained canonical. These results impose substantial constraints on the mechanism of SWI/SNF remodeling.

At the core of eukaryotic chromatin is the nucleosome, which consists of 147 bp of DNA wrapped 1.65 turns around an octamer of histone proteins¹. Even this lowest level of genomic compaction presents a strong barrier to DNA-binding cellular factors that are required for essential processes such as transcription, DNA replication, recombination and repair. Chromatin-remodeling enzymes use the energy of ATP hydrolysis to regulate accessibility of the genetic code by altering chromatin structure, and they expose specific sequences, such as promoters, to DNA-binding factors^{2–6}. The yeast SWI/SNF complex was the first remodeling enzyme to be discovered as a transcription activator⁷, and since then many homologous proteins have been found that perform similar roles in changing chromatin accessibility in higher eukaryotes, including human cells⁸.

In vitro studies have suggested that SWI/SNF-like enzymes induce formation of altered nucleosome structures by disrupting histone-DNA interactions in the canonical nucleosome structure^{9–12}. However, the state of nucleosome after the remodeling reaction is quenched remains controversial. It is still under debate as to whether remodeling generates new and stable nucleosome structures^{13–17} or whether the remodeled nucleosome resumes its canonical structure¹⁸. Furthermore, there is no consensus on whether remodeling repositions nucleosomes to well-defined locations^{13,19,20} or instead randomly redistributes them along the DNA length^{18,21}. It is even less clear how great the displacement is that results from such repositioning after each remodeling event. Some of these inconsistencies may arise from the use of mononucleosomes flanked by short DNA segments of 10–50 bp, where the ends of the DNA may have unduly influenced the outcome of the observations. Even on such short templates, the initial

canonical nucleosomes often assume multiple positions, making data interpretation even more challenging. Other experiments have been performed on longer DNA templates and used assembled nucleosomal arrays, which make high-resolution studies difficult. In addition, conventional biochemical techniques, such as nuclease-accessibility assays, often have difficulty in resolving positional from structural changes in a nucleosome.

We present a unique single-molecule approach that overcame many of these difficulties. A mononucleosome was uniquely positioned by a strong positioning element and flanked by relatively long segments of DNA (>200 bp). We unzipped the double helix of each nucleosomal DNA and probed the histone-DNA interactions sequentially by measuring the force necessary to disrupt them. The resulting linear map of the interactions along the DNA directly revealed both the position and structure of a nucleosome either unremodeled or remodeled by the yeast SWI/SNF enzyme. We focused on answering several major questions regarding the mechanism of SWI/SNF chromatin remodeling. (i) Does remodeling produce persistent altered nucleosomal structures? (ii) What is the direction of movement of a remodeled nucleosome? (iii) What is the corresponding distance of the movement? (iv) How quickly does the remodeling take place?

RESULTS

Unzipping DNA double helix to probe single nucleosomes

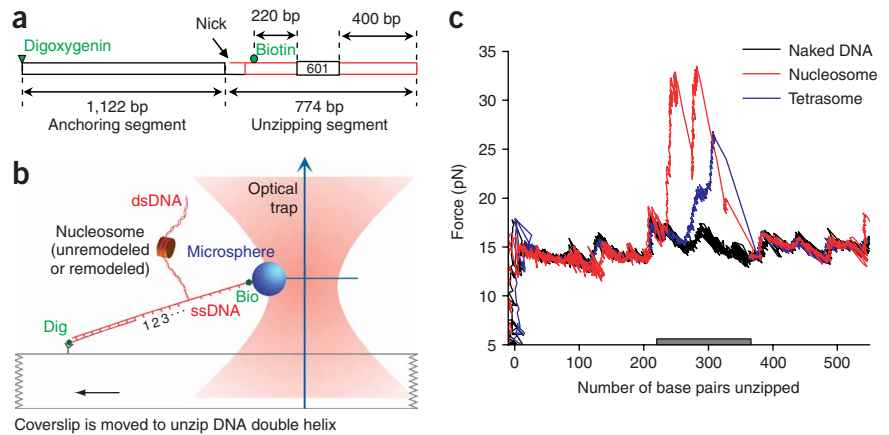
We have previously developed the unzipping technique as a versatile and powerful single-molecule method to explore protein-DNA interactions^{22–24}. In this work, we demonstrate that it provides a direct

¹Cornell University, Department of Physics, Laboratory of Atomic and Solid State Physics, Ithaca, New York 14853, USA. ²University of Massachusetts Medical School, Program in Molecular Medicine, Worcester, Massachusetts 01605, USA. ³Cornell University, Department of Molecular Biology and Genetics, Ithaca, New York 14853, USA. Correspondence should be addressed to M.D.W. (mdw17@cornell.edu).

Received 23 March; accepted 2 May; published online 28 May 2006; doi:10.1038/nsmb1102

Figure 1 Experimental setup and raw data.

(a) DNA template for single-molecule experiments consisted of two parts, separated by a nick in one DNA strand: a digoxigenin-labeled anchoring segment that always remained double stranded and a biotin-labeled unzipping segment that had its two DNA strands separated (unzipped) during experiments. The unzipping segment contained a single strong nucleosome-positioning sequence (601). (b) Nucleosomal template was suspended between the glass coverslip surface and a microsphere via a digoxigenin–anti-digoxigenin linkage at the coverslip and a biotin-streptavidin linkage at the microsphere. An optical trap was used to apply a variable force necessary to unzip through the DNA and nucleosome as the coverslip was moved away from the trapped microsphere. (c) Plotting applied force versus number of base pairs unzipped for naked DNA and DNA containing a single nucleosome or tetrasome allowed us to detect the protein-DNA interactions as they were being disrupted sequentially. Gray bar indicates the 147-bp expected 601 nucleosome position²⁶.



approach to precisely determine the locations and relative strengths of histone-DNA interactions within a single nucleosome.

We assembled histone octamers onto an 800-bp unzipping DNA segment containing the strong nucleosome-positioning sequence 601 (refs. 25,26) flanked by long random DNA stretches (Fig. 1a). A single nucleosome was located at the 601 sequence, as determined by gel-shift and enzyme-accessibility assays (data not shown). The 147-bp 601 sequence has a high affinity for the histone octamer and has been shown to position the nucleosome to a unique location on the DNA template²⁶. This resulted in a fully homogenous starting nucleosome population and allowed bidirectional nucleosome movement during remodeling.

The nucleosomal unzipping segment was ligated to an anchoring DNA segment and suspended between an optically trapped microsphere and the glass coverslip surface (Fig. 1b). The anchoring and the unzipping segments of the DNA template were joined by a single strand only; the nick in the opposite strand allowed the two DNA strands to separate when the coverslip was moved away from the optical trap. During experiments, the anchoring strand remained double stranded, whereas the unzipping strand started fully double stranded and was gradually unzipped into two single DNA strands.

The force required to unzip through a DNA molecule in the absence of proteins was sequence-dependent, with small fluctuations around 15 pN under our experimental conditions (Fig. 1c). However, a nucleosome bound to the DNA provided a strong barrier to strand separation. As the unzipping proceeded through a nucleosome, the histone-DNA bonds were disrupted sequentially with larger forces, revealing the underlying stronger interactions. Therefore, the resulting data of force versus number of base pairs unzipped served as a linear map of nucleosomal interactions along the DNA.

Characteristic disruption signature of a nucleosome

An individual nucleosome disruption showed a complex characteristic unzipping force signature with an overall shape that was highly reproducible (Figs. 1 and 2). We detected three regions of strong histone-DNA interactions, with the first two always present in the disruption signature and the third missing in most traces. The first two observed interaction regions were of similar lengths, with the second region requiring on average higher forces to unzip (Fig. 2a and

Table 1). After the first and second regions were disrupted, the nucleosome structure probably became unstable and dissociated before the last region could be probed. This was further confirmed by essentially identical disruption signatures detected by experiments that unzipped through the nucleosome from the opposite direction (data not shown). The strong histone-DNA interaction regions detected for nucleosome disruptions always occurred at essentially identical positions along the DNA. For convenience, we define the nucleosome position as the mean location of interaction region 1 (see Methods). The precision of nucleosome position determination was 2.6 bp, calculated by fitting a gaussian function to the position histogram of nucleosomes assembled onto the 601 sequence (Fig. 2b and Supplementary Fig. 1 online).

By comparing our results with crystallographic nucleosome structure data²⁷, we correlated the unzipping signature with observed histone-DNA contacts. The two high-force regions occurred within the first half of the nucleosome (Fig. 1c, gray bar), up to and sometimes a little beyond the nucleosome center, which is the position of the dyad at 294 bp unzipped. Therefore, the second and relatively stronger interaction region is probably due to the histone-DNA interactions of histones H3 and H4 that occur around the nucleosomal dyad. The first strong interaction region as well as the third region were centered ~50 bp away from the dyad position and are probably due to the H2A-H2B interactions expected within those regions. Notably, these three regions of strong interactions are also consistent with our previous single-molecule studies of nucleosome stability: by stretching a nucleosomal DNA end to end, we mechanically disrupted individual nucleosomes, and the stage-wise DNA release indicated the presence of these three strong interactions^{28–30}.

To determine whether our technique could detect changes in nucleosome structure, we unzipped through tetrasomes, consisting of assembled H3-H4 histone tetramer only. The tetrasomes showed a considerably different unzipping signature with a single high-force region (Fig. 1c and Table 1). This region's length was comparable to the length of each of the first two interaction regions in a nucleosome. However, tetrasome disruptions occurred at measurably lower unzipping forces, indicating weaker underlying histone-DNA interactions. The single interaction region within the tetrasome must be due to H3-H4 contacts that are more weakly bound in this configuration than in a nucleosome.

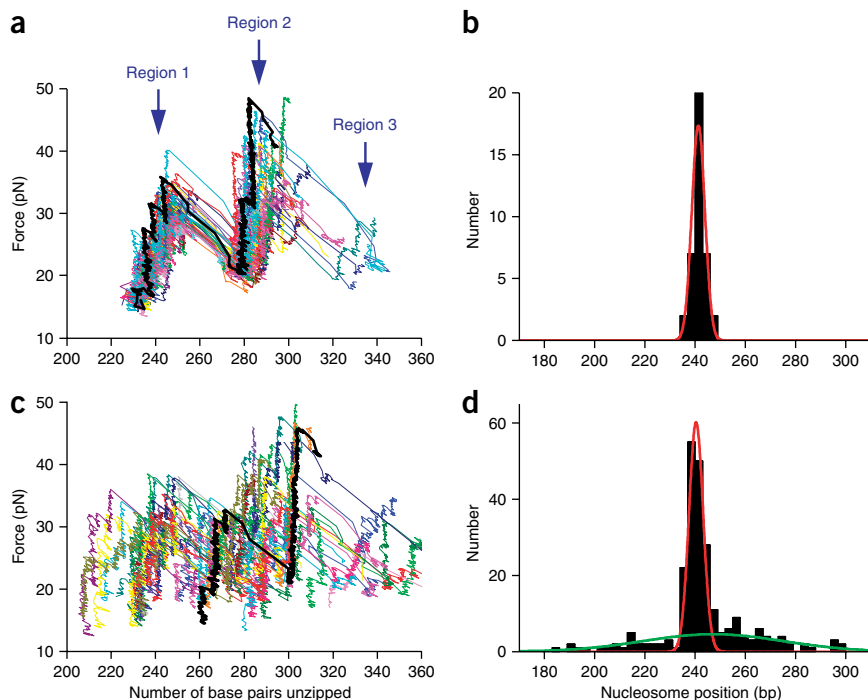


Figure 2 Unzipping through unremodeled and remodeled nucleosomes. **(a)** Disruption force versus number of base pairs unzipped for 30 unremodeled data curves. A single representative curve is highlighted in black. **(b)** Histogram of unremodeled nucleosome positions on the DNA. A nucleosome position is defined as the mean position of interaction region 1 (see **Fig. 2a**). Data (black) and their gaussian fit (red) are shown. The distribution is centered at 241 bp with an s.d. of 2.6 bp. **(c)** Disruption force versus number of base pairs unzipped for 30 data curves obtained after SWI/SNF remodeling. A single representative curve is highlighted in black. **(d)** Histogram of remodeled nucleosome positions on the DNA after remodeling reaction times <1 min. Data (black) and their fit to two gaussian functions (red and green) are shown. Red fit curve represents the nucleosome population that remained at the original 601 position (unremodeled; center = 240 bp, s.d. = 2.8 bp); green curve corresponds to those moved by the action of SWI/SNF (remodeled; center = 247 bp, s.d. = 28 bp).

plus the SWI/SNF with and without ATP did not show any disruption peaks. Together, these results indicate that the disruption signature observed after remodeling can be

attributed wholly to histone-DNA interactions, and SWI/SNF was probably removed during sample preparation (see Methods).

We observed that nucleosome disruptions retain their overall distinctive shape after remodeling—that is, at least two strong histone-DNA interaction regions are always present in the disruption signature (compare highlighted curves in **Fig. 2a,c**; also see **Supplementary Fig. 2** online). Characteristic disruption parameters of unremodeled and remodeled nucleosomes, summarized in **Table 1**, show comparable disruption lengths, total disruption times and maximum forces. Thus, we conclude that, under our experimental conditions, SWI/SNF remodeling does not alter the overall nucleosome structure: the histone octamer remains intact and the overall strengths and positions of histone-DNA interactions within the nucleosome are essentially unchanged.

Nucleosome positions after SWI/SNF remodeling

The main consequence of remodeling we detected was bi-directional nucleosome movement along the DNA (**Fig. 2c**). Plotting nucleosome position for all samples that were allowed to react for <1 min reveals two distinct populations (**Fig. 2d**). One population remained at the original 601 position without measurable changes in either the average nucleosome position or its distribution width. The other population retained approximately the same average position, but the nucleosomes were spread out considerably, with a standard deviation of 28 bp.

Increasing remodeling reaction times had two consequences. First, the fraction of nucleosomes that remained at the original 601 position decreased, whereas the width of

Nucleosome structure after SWI/SNF remodeling

We used the unzipping technique to probe the structures of individual nucleosomes after SWI/SNF remodeling. SWI/SNF remodeling reactions were prepared as described in Methods. After remodeling, nucleosomes were tethered in the single-molecule chamber (**Fig. 1b**) and unzipped through in a way identical to unremodeled nucleosomes. We assume that nucleosome positions did not change owing to thermal mobility after the remodeling reaction was stopped; higher temperatures are generally required for nucleosome thermal motion within our experimental time frame^{19,31}. No additional force peaks were observed for the remodeled samples compared to the unremodeled nucleosome data. Also, control samples made with naked DNA

Table 1 Comparison of structures of unremodeled nucleosomes, remodeled nucleosomes and tetrasomes

| | Unremodeled nucleosomes | Remodeled nucleosomes |
|--|-------------------------|-----------------------|
| Number of data files | 38 | 148 |
| Total disruption time (s) | 3.9 ± 0.8 | 3.6 ± 0.9 |
| Mean number of interaction regions detected | 2.1 ± 0.3 | 2.1 ± 0.5 |
| Interaction region 1 length (bp) | 25 ± 5 | 18 ± 7 |
| Interaction region 1 maximum force (pN) | 31 ± 2 | 31 ± 6 |
| Interaction region 2 length (bp) | 20 ± 8 | 19 ± 8 |
| Interaction region 2 maximum force (pN) | 37 ± 7 | 37 ± 6 |
| Distance between centers of regions 1 and 2 (bp) | 45 ± 6 | 41 ± 7 |
| | Tetrasome | |
| Number of data files | 20 | |
| Total disruption time (s) | 1.2 ± 0.4 | |
| Mean number of interaction regions detected | 1.1 ± 0.4 | |
| Interaction region length (bp) | 18 ± 7 | |
| Interaction region maximum force (pN) | 25 ± 2 | |

Characteristic disruption parameters for unremodeled nucleosomes, remodeled nucleosomes and tetrasomes. The remodeled nucleosomes column includes data from only those nucleosomes that were moved from the original 601 position by ±6 bp or more. Errors show s.d.

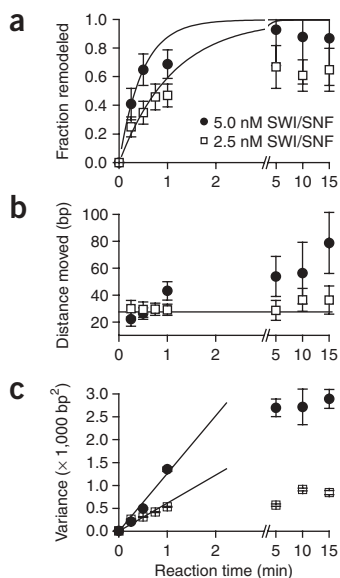


Figure 3 Kinetics of SWI/SNF-catalyzed nucleosome remodeling. (a) Fraction of nucleosomes moved versus reaction time. Moved nucleosome fractions for 5 nM and 2.5 nM SWI/SNF were calculated from nucleosome-position distributions as described in Methods. Short-time data (<1 min) were fit to the exponential form $1 - e^{-(t/\tau)}$ resulting in time constant τ values of 28.5 ± 5.0 s and 66.5 ± 5.3 s for 5 nM and 2.5 nM SWI/SNF, respectively. The fraction for long reaction times was underestimated (see Methods). (b) Distance moved, defined as the s.d. of the positions of remodeled nucleosomes, versus reaction time. Single remodeling event-characteristic distance $\lambda = 28 \pm 3$ bp (line) was obtained by averaging all data for remodeling reaction times <1 min. (c) Variances of nucleosome positions (unremodeled and remodeled) versus reaction time. Linear fits to data of reaction times <1 min are shown; fit slopes are $610 \pm 70 \text{ bp}^2 \text{ min}^{-1}$ and $1,260 \pm 100 \text{ bp}^2 \text{ min}^{-1}$ for 5.0 nM and 2.5 nM SWI/SNF, respectively. In **a–c**, error bars show s.e.m.

its distribution was unchanged. Second, both the nucleosome fraction in the other population and the distribution width of this population increased with time and also with SWI/SNF concentration. After long reaction times ($\gg 1$ min), the two populations were no longer distinguishable. These results suggest that the population represented by the narrow distribution around the original 601 position in **Figure 2d** was comprised of nucleosomes that were not remodeled under our experimental conditions, whereas the other population's nucleosomes were moved along the DNA by the action of SWI/SNF.

Kinetics of nucleosome remodeling

We determined the kinetic parameters of nucleosome motion during remodeling by measuring nucleosome position distributions at different remodeling reaction times. A single remodeling event is defined here as a cycle that includes SWI/SNF binding, remodeling and detachment from the nucleosomal DNA. **Figure 3a** shows the fraction of remodeled nucleosomes as a function of reaction time for two SWI/SNF concentrations. Our calculation of the remodeled fraction (see Methods) is more accurate for short times, but underestimates this fraction for long times, when multiple remodeling events may have occurred. Therefore, remodeling-event parameters were calculated using only the data from short reaction times (<1 min), when the majority of nucleosomes were not remodeled and the remainder were probably remodeled only once. For short

reaction times, nucleosomes were found to be remodeled at an event rate proportional to SWI/SNF concentration, with a single remodeling event-characteristic times (τ) of ~ 1 and 0.5 min at 2.5 and 5.0 nM of SWI/SNF, respectively. This indicates that the catalytic efficiency of the enzyme (k_{cat}/K_m) is $\sim 0.4 \text{ min}^{-1}$ per nM SWI/SNF, assuming that it follows Michaelis-Menten enzyme kinetics and that the K_m is greater than 5 nM.

The single remodeling event-characteristic distance $\lambda = 28$ bp was calculated as the standard deviation of the positional distribution of the remodeled fraction at short reaction times (<1 min) and was a measure of the characteristic distance that the remodeled nucleosomes moved with each remodeling event. Over this time range, the average distance moved remained constant (**Fig. 3b**) while the fraction of remodeled nucleosomes increased (**Fig. 3a**). This confirms that, during the 1-min time scale, primarily single remodeling events took place for the SWI/SNF concentrations used here. Longer reaction times allowed multiple remodeling events, and the distance moved increased as the nucleosomes spread further along the DNA.

We investigated whether the first and subsequent remodeling events follow identical kinetics with the same event-characteristic time τ and event-characteristic distance λ . If so, nucleosome position after remodeling should follow a simple random walk, with the variance σ^2 in the position distribution increasing linearly with reaction time t : $\sigma^2 = (\lambda^2 / \tau)t$. **Figure 3c** shows σ^2 versus t for two different SWI/SNF concentrations. For $t \leq 1$ min, where predominantly single remodeling events occurred, linear relations were indeed observed, with slopes of 610 ± 70 and $1,260 \pm 100 \text{ bp}^2 \text{ min}^{-1}$ for 2.5 and 5.0 nM SWI/SNF, respectively. Within experimental uncertainties, these slopes are in good agreement with the expected slopes of 710 ± 160 and $1,630 \pm 440 \text{ bp}^2 \text{ min}^{-1}$ based on the measured τ and λ values derived from **Figure 3a,b**. However, for $t > 1$ min, σ^2 starts to level off, deviating from the linear relation of a random walk. This means that, after the first remodeling event, nucleosomes were more likely to remain in the vicinity of the original 601 position rather than to be distributed randomly along the entire DNA template. This effect is most probably caused by the high nucleosome affinity of the 601 sequence compared with the random DNA sequence of the rest of our template, indicating that DNA sequence can have a role in nucleosome positioning after remodeling. In other words, nucleosome remodeling that tends to spread out nucleosomes along the DNA might compete with the tendency of the 601 element to uniquely position nucleosomes.

DISCUSSION

This study presents a high-resolution approach that directly probes the strong interactions within a nucleosome by unzipping a single DNA double helix. This approach complements our previous single-molecule experiments, in which nucleosomal DNA was stretched from end to end^{28–30}. An unzipping experiment detects the absolute locations of the histone-DNA interactions along the DNA sequence, whereas a stretching experiment detects the relative locations of the interactions. The unzipping experiments directly detected the locations of three regions of strong interactions within a nucleosome; these locations were previously inferred from our stretching experiments.

This study showed that both unremodeled and remodeled nucleosomes had nearly identical complex disruption signatures during unzipping. In contrast, the disruption signature of a tetrasome was considerably different from that of a nucleosome. These data together provide strong evidence that a nucleosome resumes its canonical structure after remodeling. It is possible that structural

alterations may have been present within the part of the nucleosome that was not probed by our experiments. However, half or more of the histone-DNA contact surface was probed in all detected disruptions, and nucleosomes unzipped in the opposite direction also showed essentially identical disruption signatures. This supports the argument that no substantial structural changes of the remodeled nucleosomes were stable enough to be detected under our experimental conditions.

These results do not imply that the nucleosome structure is unaltered during remodeling; instead, they suggest that any such altered structures are transient and unstable upon removal of SWI/SNF or ATP. They also suggest that remodeling does not result in a loss of H2A-H2B dimer. Although dimer loss has previously been suggested as an outcome of SWI/SNF remodeling^{32–34}, our results indicate that such loss, if any, was rare under our experimental conditions and therefore may not be a universal feature of remodeling.

We also observed that SWI/SNF-mediated remodeling resulted in bi-directional movement of nucleosomes along the DNA template. We did not observe relocation of remodeled nucleosomes to specific locations; instead, they showed a continuous distribution around their original position on the DNA. This distribution had a standard deviation of ~ 28 bp after one remodeling event, and remodeling events occurred with a catalytic efficiency of 0.4 min^{-1} per nM SWI/SNF. These results provide the most direct measurements of the direction of movement and location distribution of remodeled nucleosomes yet reported, and they yield a kinetic parameter that is difficult to extract using conventional biochemical methods.

These observations impose important constraints on possible mechanisms of remodeling. Remodeled nucleosomes were observed to move in opposite directions with nearly equal probabilities. This indicates that SWI/SNF was able to bind in either orientation relative to the DNA sequence, even though the sequence used was not palindromic. The characteristic 28-bp distance moved per remodeling event indicates that changes of the nucleosome structure during SWI/SNF remodeling, such as possible loop or bulge formation, are on this order of magnitude. We did not observe a unique distance moved but rather a continuous distribution of distances. This could mean that nucleosome structure may be altered to different extents during remodeling or, alternatively, that the structure is always altered to the same extent but then relaxes to a distribution of positions upon resuming the canonical structure.

METHODS

Nucleosomal template. The DNA construct used in unzipping experiments was designed as two separate segments (Fig. 1a). The 1.1-kb anchoring segment was prepared by PCR from plasmid pRL574 (ref. 35) using a digoxigenin (dig)-labeled primer and then digested with BstXI (NEB) to produce a ligatable overhang. The 0.8-kb unzipping fragment was prepared by PCR from plasmid 601 (ref. 25) using a biotin-labeled primer and then digested with BstXI and dephosphorylated using CIP (NEB) to introduce a nick into the final DNA template. Nucleosomes were assembled from purified HeLa histones onto the unzipping fragment by a well-established salt dialysis method³⁶. The two segments were joined by ligation immediately before use. This produced the complete template, which was labeled with a single dig tag on one end and a biotin tag located 7 bp after the nick in one DNA strand.

Chromatin remodeling. Yeast SWI/SNF was purified as described³⁷. Remodeling reactions containing 5 nM assembled nucleosomes, 5 nM or 2.5 nM purified yeast SWI/SNF and 1 mM ATP in remodeling buffer (10 mM Tris-HCl

(pH 8.0), 100 mM NaCl, 7 mM MgCl₂, 2 mM DTT, 0.1 mg ml⁻¹ BSA) were incubated at 37 °C for specified durations. The reactions were stopped by addition of 10 mM EDTA and placed on ice for 10 min to a few hours before being used in preparing single-molecule samples. No dependence of the unzipping results on this time length was observed. Before addition to the single-molecule sample chamber, the remodeling reaction was diluted by a factor of 10 in dilution buffer (10 mM Tris-HCl (pH 7.5), 1 mM EDTA, 150 mM NaCl, 1 mM DTT, 3% (v/v) glycerol, 0.1 mg ml⁻¹ BSA).

Data acquisition and conversion. Single-molecule sample preparation was performed according to protocols similar to those previously described^{22,28}. Briefly, after microspheres were tethered to the coverslip surface by DNA (Fig. 1a,b), the sample chamber was rinsed twice with 5× chamber volumes of sample buffer (10 mM Tris-HCl (pH 7.5), 1 mM EDTA, 100 mM NaCl, 1.5 mM MgCl₂, 1 mM DTT, 3% (v/v) glycerol, 0.02% (v/v) Tween 20, 2 mg ml⁻¹ BSA). All single-molecule measurements were performed in this sample buffer. Note that the process of tethering the microspheres to the coverslip and subsequent rinsing should effectively remove any proteins not bound to the tethered DNA or chamber surfaces.

A single-molecule optical trapping setup was used to unzip the DNA template by moving the coverslip horizontally away from the optical trap. When a bound protein was encountered, a computer-controlled feedback loop increased the applied load linearly with time (8 pN s^{-1}) as necessary to unzip through the protein-DNA interactions²³. Data were digitized at 12 kHz and boxcar-averaged to 60 Hz. The acquired data signals were converted into force and number of base pairs unzipped as described²². Additionally, the force-versus-base pairs unzipped curve was aligned to a theoretical DNA unzipping curve³⁸ (see **Supplementary Fig. 1**), improving positional precision to 2.6 bp for nucleosome positions (Fig. 2b).

We found that, for nucleosomal samples, the last 100–200 bp of the unzipping curves did not always show the expected naked DNA shape. Instead, in some traces we observed random high-force peaks that were not present when unzipping naked DNA. We attribute this effect to nonspecific interactions between the end of the DNA and the histone proteins removed from the disrupted nucleosome. To avoid possible contamination of nucleosome-disruption data from these nonspecific interactions, only data that showed at least 100 bp of naked DNA unzipping pattern after a disruption were used for analysis.

Data analysis. A nucleosome position was defined as the mean location of the data points in interaction region 1, which is clearly distinguishable from region 2, as there were very few data points between the two regions (Fig. 2a). The fraction of nucleosomes moved during remodeling was determined from nucleosome-position histograms (similar to that shown in Fig. 2d) in two ways. For data at short reaction times (< 1 min) and for each time point, a maximum-likelihood method³⁹ was used to determine the best fit to a sum of two gaussian functions corresponding to unremodeled and remodeled nucleosome populations. This fit yielded the fraction of nucleosomes that were remodeled. As the remodeled fraction had a mean near the original 601 position, we defined the characteristic distance moved for the remodeled nucleosomes as the standard deviation of their position distribution. The error bars of the fraction remodeled and distance moved were determined by the uncertainties in the fit parameters. Data from long reaction times (> 1 min) no longer showed two distinct position distributions, and we defined remodeled nucleosomes as those moved at least 6 bp from the original 601 position. The moved fractions and distances were then determined directly from the numbers of unremodeled and remodeled nucleosomes, and their error bars show s.e.m.

Note: Supplementary information is available on the Nature Structural & Molecular Biology website.

ACKNOWLEDGMENTS

We thank M. Hall for help with data analysis, L. Bai, J. Jin, B. Brower-Toland, R.M. Fulbright, D. Wacker, J. Tang, V. Elser and J.P. Sethna for helpful suggestions, members of the Wang laboratory for critical comments on the manuscript, J. Widom (Northwestern University) and R. Landick (University of Wisconsin) for gifts of plasmids and the National Cell Culture Center for HeLa cells. This research was supported by US National Institutes of Health grants to

J.T.L, C.L.P. and M.D.W and the Keck Foundation's Distinguished Young Scholar Award to M.D.W.

COMPETING INTERESTS STATEMENT

The authors declare that they have no competing financial interests.

Published online at <http://www.nature.com/nsmb/>

Reprints and permissions information is available online at <http://npg.nature.com/reprintsandpermissions/>

- Davey, C.A., Sargent, D.F., Luger, K., Maeder, A.W. & Richmond, T.J. Solvent mediated interactions in the structure of the nucleosome core particle at 1.9 Å resolution. *J. Mol. Biol.* **319**, 1097–1113 (2002).
- Kingston, R.E. & Narlikar, G.J. ATP-dependent remodeling and acetylation as regulators of chromatin fluidity. *Genes Dev.* **13**, 2339–2352 (1999).
- Kornberg, R.D. & Lorch, Y. Twenty-five years of the nucleosome, fundamental particle of the eukaryote chromosome. *Cell* **98**, 285–294 (1999).
- Vignali, M., Hassan, A.H., Neely, K.E. & Workman, J.L. ATP-dependent chromatin-remodeling complexes. *Mol. Cell. Biol.* **20**, 1899–1910 (2000).
- Smith, C.L. & Peterson, C.L. ATP-dependent chromatin remodeling. *Curr. Top. Dev. Biol.* **65**, 115–148 (2005).
- Becker, P.B. & Horz, W. ATP-dependent nucleosome remodeling. *Annu. Rev. Biochem.* **71**, 247–273 (2002).
- Winston, F. & Carlson, M. Yeast SNF/SWI transcriptional activators and the SPT/SIN chromatin connection. *Trends Genet.* **8**, 387–391 (1992).
- Sudarsanam, P. & Winston, F. The Swi/Snf family nucleosome-remodeling complexes and transcriptional control. *Trends Genet.* **16**, 345–351 (2000).
- Bazett-Jones, D.P., Cote, J., Landel, C.C., Peterson, C.L. & Workman, J.L. The SWI/SNF complex creates loop domains in DNA and polynucleosome arrays and can disrupt DNA-histone contacts within these domains. *Mol. Cell. Biol.* **19**, 1470–1478 (1999).
- Schnitzler, G.R. *et al.* Direct imaging of human SWI/SNF-remodeled mono- and polynucleosomes by atomic force microscopy employing carbon nanotube tips. *Mol. Cell. Biol.* **21**, 8504–8511 (2001).
- Aoyagi, S. *et al.* Nucleosome remodeling by the human SWI/SNF complex requires transient global disruption of histone-DNA interactions. *Mol. Cell. Biol.* **22**, 3653–3662 (2002).
- Narlikar, G.J., Phelan, M.L. & Kingston, R.E. Generation and interconversion of multiple distinct nucleosomal states as a mechanism for catalyzing chromatin fluidity. *Mol. Cell* **8**, 1219–1230 (2001).
- Kassabov, S.R., Zhang, B., Persinger, J. & Bartholomew, B. SWI/SNF unwraps, slides, and rewraps the nucleosome. *Mol. Cell* **11**, 391–403 (2003).
- Fan, H.Y., He, X., Kingston, R.E. & Narlikar, G.J. Distinct strategies to make nucleosomal DNA accessible. *Mol. Cell* **11**, 1311–1322 (2003).
- Cote, J., Peterson, C.L. & Workman, J.L. Perturbation of nucleosome core structure by the SWI/SNF complex persists after its detachment, enhancing subsequent transcription factor binding. *Proc. Natl. Acad. Sci. USA* **95**, 4947–4952 (1998).
- Schnitzler, G., Sif, S. & Kingston, R.E. Human SWI/SNF interconverts a nucleosome between its base state and a stable remodeled state. *Cell* **94**, 17–27 (1998).
- Lorch, Y., Cairns, B.R., Zhang, M. & Kornberg, R.D. Activated RSC-nucleosome complex and persistently altered form of the nucleosome. *Cell* **94**, 29–34 (1998).
- Jaskelioff, M., Gavin, I.M., Peterson, C.L. & Logie, C. SWI-SNF-mediated nucleosome remodeling: role of histone octamer mobility in the persistence of the remodeled state. *Mol. Cell. Biol.* **20**, 3058–3068 (2000).
- Flaus, A. & Owen-Hughes, T. Dynamic properties of nucleosomes during thermal and ATP-driven mobilization. *Mol. Cell. Biol.* **23**, 7767–7779 (2003).
- Zofall, M., Persinger, J., Kassabov, S.R. & Bartholomew, B. Chromatin remodeling by ISW2 and SWI/SNF requires DNA translocation inside the nucleosome. *Nat. Struct. Mol. Biol.* **13**, 339–346 (2006).
- Whitehouse, I. *et al.* Nucleosome mobilization catalysed by the yeast SWI/SNF complex. *Nature* **400**, 784–787 (1999).
- Koch, S.J., Shundrovsky, A., Jantzen, B.C. & Wang, M.D. Probing protein-DNA interactions by unzipping a single DNA double helix. *Biophys. J.* **83**, 1098–1105 (2002).
- Koch, S.J. & Wang, M.D. Dynamic force spectroscopy of protein-DNA interactions by unzipping DNA. *Phys. Rev. Lett.* **91**, 028103 (2003).
- Jiang, J. *et al.* Detection of high-affinity and sliding clamp modes for MSH2-MSH6 by single-molecule unzipping force analysis. *Mol. Cell* **20**, 771–781 (2005).
- Lowary, P.T. & Widom, J. New DNA sequence rules for high affinity binding to histone octamer and sequence-directed nucleosome positioning. *J. Mol. Biol.* **276**, 19–42 (1998).
- Thastrom, A., Bingham, L.M. & Widom, J. Nucleosomal locations of dominant DNA sequence motifs for histone-DNA interactions and nucleosome positioning. *J. Mol. Biol.* **338**, 695–709 (2004).
- Luger, K., Mader, A.W., Richmond, R.K., Sargent, D.F. & Richmond, T.J. Crystal structure of the nucleosome core particle at 2.8 Å resolution. *Nature* **389**, 251–260 (1997).
- Brower-Toland, B.D. *et al.* Mechanical disruption of individual nucleosomes reveals a reversible multistage release of DNA. *Proc. Natl. Acad. Sci. USA* **99**, 1960–1965 (2002).
- Brower-Toland, B. & Wang, M.D. Use of optical trapping techniques to study single-nucleosome dynamics. *Methods Enzymol.* **376**, 62–72 (2004).
- Brower-Toland, B. *et al.* Specific contributions of histone tails and their acetylation to the mechanical stability of nucleosomes. *J. Mol. Biol.* **346**, 135–146 (2005).
- Meersman, G., Pennings, S. & Bradbury, E.M. Mobile nucleosomes—a general behavior. *EMBO J.* **11**, 2951–2959 (1992).
- Cote, J., Quinn, J., Workman, J.L. & Peterson, C.L. Stimulation of GAL4 derivative binding to nucleosomal DNA by the yeast SWI/SNF complex. *Science* **265**, 53–60 (1994).
- Bruno, M. *et al.* Histone H2A/H2B dimer exchange by ATP-dependent chromatin remodeling activities. *Mol. Cell* **12**, 1599–1606 (2003).
- Vicent, G.P. *et al.* DNA instructed displacement of histones H2A and H2B at an inducible promoter. *Mol. Cell* **16**, 439–452 (2004).
- Schafer, D.A., Gelles, J., Sheetz, M.P. & Landick, R. Transcription by single molecules of RNA polymerase observed by light microscopy. *Nature* **352**, 444–448 (1991).
- Lee, K.-M. & Narlikar, G. Assembly of nucleosomal templates by salt dialysis. in *Current Protocols in Molecular Biology* Vol. 3 (eds. Ausubel, F.A. *et al.*) 21.6.3 (Wiley, New York, 2001).
- Smith, C.L., Horowitz-Scherer, R., Flanagan, J.F., Woodcock, C.L. & Peterson, C.L. Structural analysis of the yeast SWI/SNF chromatin remodeling complex. *Nat. Struct. Mol. Biol.* **10**, 141–145 (2003).
- Bockelmann, U., Essevaz-Roulet, B. & Heslot, F. DNA strand separation studied by single molecule force measurements. *Phys. Rev. E* **58**, 2386–2394 (1998).
- Orear, J. Notes on statistics for physicists. (Laboratory for Nuclear Studies report CLNS 82/511, Cornell University, New York, 1982).